Active Suspension for the Control of Planar Vehicle Dynamics

Scott Varnhagen, Olugbenga Moses Anubi, Zachary Sabato and Donald Margolis
School of Mechanical and
Aerospace Engineering
University of California
Davis, California 95616
Email: svarnhagen@ucdavis.edu

Abstract—**A novel method of actuating an active suspension system for the control of planar vehicle dynamics is proposed. Active suspension forces are applied in such a way that their effect on the chassis heave-pitch-roll dynamics is negligible. Instead, their impact is restricted to the generation of longitudinal and lateral tire forces, resulting in controllability of planar vehicle dynamics. An optimal control strategy is proposed to benchmark the system performance, relying on unknowable tire information. The strategy's robustness to error in tire parameters is formulated analytically, and it is shown that estimates of these parameters are sufficient for stable operation. Based on this result, a sub-optimal control routine is developed using only estimable signals. The result is a realizable control strategy which utilizes active suspension components to stabilize planar vehicle dynamics without upsetting chassis dynamics.**

I. INTRODUCTION

Active Suspension: Active suspension technology has been broadly investigated for many decades [1]–[3]. Where large ground inputs are common, such as military and industrial vehicles operating off-road, the ability of active suspensions to reduce operator and cargo accelerations is very valuable. Conversely, active suspension has failed to gain widespread adoption in the consumer automotive sector for ride control, where the average roadway is significantly smoother. The necessary hardware and power costs result in an unappealing value proposition, especially when compared to the performance of semi-active algorithms like Skyhook damping [4].

Active suspension can inject forces at each chassis corner over a range of operating energies; whereas their performance is weak at wheel-hop frequencies due to excess power usage, coordinating the suspension for normal force control may have a much lower requirement on bandwidth while still achieving a stabilizing effect on vehicle dynamics.

Normal Force Variation: Research conducted by Margolis and Blank exposed how normal force variation owing to road unevenness impacts road-holding and lateral dynamics [5]. It is shown that the strong effect which normal force variation has on lateral behavior is significantly affected by forward speed and frequency content of the roadway input.

Additionally, work completed by Shim and Margolis has shown that, through the use of decoupled proportional-derivative controllers, normal forces can be modulated based on a yaw rate error derived from a model-reference vehicle [6].

The algorithm used is based on a heuristic relating dynamic oversteer and understeer; the authors indicate that a multiple-input multiple-output controller could potentially cope with the intrinsic dynamic coupling present in normal force generation. Furthermore, no consideration was explicitly made for the normal force actuators' effect on chassis motion.

This work demonstrates an active suspension control philosophy capable of manipulating tire normal loading and associated resultant force generation. This manipulation allows for the total lateral force as well as total yaw-moment generated by the tires to be manipulated during vehicle cornering. The implication is that the planar dynamics of the vehicle may be augmented by an intelligent control of the active suspension system. An additional constraint imposed on the active suspension system is that its control effort should not significantly modify the chassis attitude. It is assumed that the roll, pitch and heave dynamics of the chassis have been made desirable by the suspension designer utilizing passive and active suspension components. Thus, the novel active suspension control philosophy introduced in this work effects planar vehicle dynamics without upsetting chassis dynamics.

Paper Organization: Components of the system model used in this work are discussed in Section II. Section III details the optimal and sub-optimal control allocation architectures. Simulation results are presented in Section IV. Section V reviews the paper's findings and draws conclusions.

II. SYSTEM MODEL

A. Vertical Vehicle Dynamics

For simulation purposes, the active suspension forces are injected in between the sprung and un-sprung masses at each suspension attachment location. When the controlled input is positive, this has the effect of accelerating that corner of the chassis upward and the tire toward the ground (increasing the contact patch normal force). The desired change in normal loading ΔF_z is related to the required actuator force F_s through the motion ratio M:

$$F_{s_{ij}} = \frac{\Delta F_{z_{ij}}}{M_{ij}^2}. \tag{1}$$

Motion ratio [7] is defined as the ratio between wheel travel and suspension travel and can be fully determined off-line through analysis of suspension geometry. In reality, changes in active suspension force F_s would be dynamically transmitted to changes in normal loading ΔF_z. These dynamics would include chassis motion, as well as unsprung mass motion. However, as will be discussed in Section III-A, an active suspension control law is developed which does not influence chassis motion. Therefore the only dynamics invoked by the application of active suspension forces are those of the unsprung masses [8]. These dynamics are generally well damped, and occur with a bandwidth in the realm of the wheel-hop frequency, approximately $10Hz$ [9]. Conversely, planar vehicle dynamics involve chassis motion and unfold at a much lower frequency. For these reasons, it is appropriate to neglect the dynamics involved during the generation of normal force as a result of active suspension force, resulting in the relationship presented in Eqn. (1).

The electrical and dynamic mechanical properties of the active suspension actuators have been omitted in this work. In lieu of these implicit constraints on force generation, rate and magnitude limits are imposed to both ensure physical realizability and allow for eventual selection of appropriate hardware.

B. Tire Force Generation

It is the goal of this work to control planar vehicle dynamics using active suspension elements for actuation. As shown in Eqn. (1), forces injected by the active suspension elements correspond to changes in tire normal loading. This section focuses on the relationship between tire normal loading and corresponding longitudinal and lateral force generation. With this knowledge, a control methodology is developed in subsequent sections which augments tire normal loading to obtain control over planar vehicle dynamics.

In a simple sense, tires can be thought of as multi-dimensional springs. Their deflection in the longitudinal direction is measured by slip-ratio, σ and in the lateral direction by slip-angle α. Operating with relatively small deformations the tire generates longitudinal and lateral forces in approximately linear proportion to σ and α respectively. However, the maximum resultant force that a tire may generate is a function of its normal loading and the coefficient of friction between the tire and the road surface. Therefore, at larger σ and α, tire behavior exhibits saturation, a non-linear phenomenon. The Pacejka Magic Formula (MF) is used to model the constitutive relationship by which tires generate force [10]. The MF consists of arctangent functions with parameters obtained by fitting the model with empirical tire test data.

In this work, the MF is used to determine how changes in normal loading will effect longitudinal and lateral force generation based on the current operating state of the tire. This idea is illustrated in Figure 1 for a tire operating with a slip-ratio of $\sigma = 0.01$ and slip-angle of $\alpha = 4^o$. The plot shows longitudinal and lateral tire force generation with respect to normal loading and is generated using the MF.
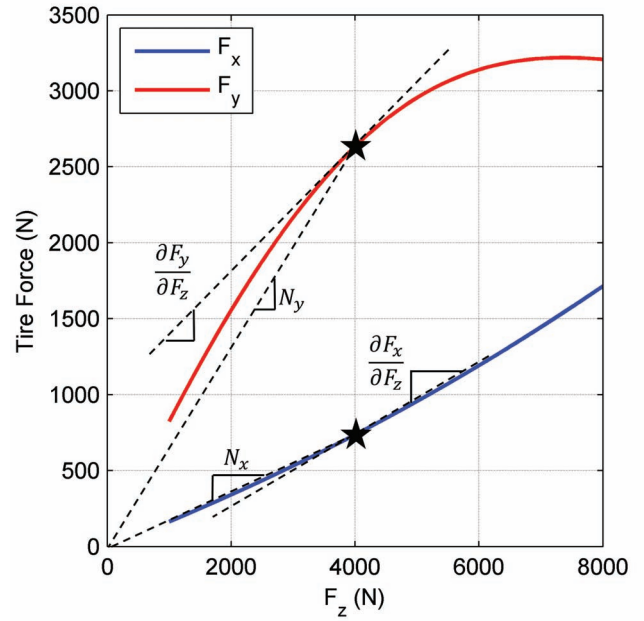

Fig. 1. Lateral and Longitudinal Force Generation with Respect to Normal Loading for Tire Operating with $\alpha = 4^o$ and $\sigma = 0.01$

Assuming that the tire is currently operating with a normal loading of $F_z = 4000N$, represented by $\star$, the change in lateral and longitudinal force generation can be determined in this neighborhood by differentiating the MF with respect to normal loading, shown on the figure as $\frac{\partial F_y}{\partial F_z}$ and $\frac{\partial F_x}{\partial F_z}$. This knowledge of tire force generation with respect to changes in normal loading is used by the optimal control allocation problem described in Section III-A1.

This controller is not practically realizable as the partial derivatives described could not be known in real time due to uncertainty in tire and road parameters, but is developed to serve as a benchmark for the sub-optimal pragmatic controller developed in this work. The partial derivatives, which provide an affine representation of change in planar force with respect to change in normal loading are approximated by the linear parameters N_y and N_x. These linear parameters are defined in Eqn. (2) and presented in Figure 1. Unlike the partial derivatives discussed above, the linear parameters consist of real time estimable quantities, and thus can be used by a practical controller. Literature describing the estimation of longitudinal, lateral and normal tire forces can be found in [11]. A suboptimal control allocation problem, utilizing these estimable linear variables as opposed to the indeterminate partial derivatives is discussed in Section III-A2.

$$N_y = \frac{F_y}{F_z}, N_x = \frac{F_x}{F_z} \qquad (2)$$

C. Planar Vehicle Dynamics

Figure 2 depicts the handling model which is an extension of the two degree-of-freedom bicycle model. To augment the traditional handling model, weight transfer effects are included
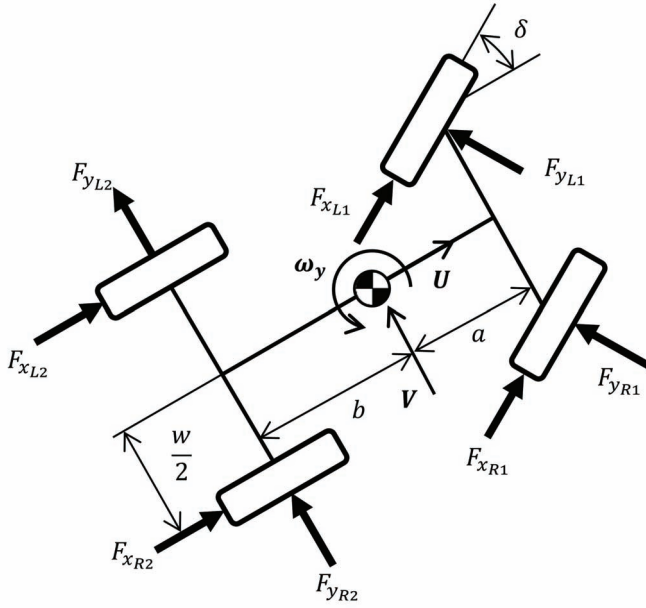
4086

Fig. 2. Planar Free Body Diagram of Vehicle

by considering the vertical center of gravity location. Thus the model accounts for change in normal loading, and is applicable to our study of the effect of normal loading on planar vehicle dynamics. The center of gravity is placed in the fore aft direction by the parameters a and b and is centered laterally between the vehicle track width w. The tire at each corner of the vehicle can generate lateral and longitudinal forces F_y and F_x. The vehicle exhibits body fixed longitudinal velocity U and lateral velocity V. Additionally, the vehicle may rotate in the plane with yaw-rate ω_y. The front wheels of the vehicle may be steered by angle δ.

The bicycle and handling model of planar vehicle dynamics assume a constant forward velocity U, and thus it is assumed that tire forces in the longitudinal direction are negligible. The two models have only two states, lateral velocity V and yaw-rate ω_y, whose dynamical equations are generated by a summation of the lateral forces and moments in Figure 2, resulting in the equations provided in (3) and (4). The term $(\dot{V} + \omega_y U)$ represents body fixed lateral acceleration. m represents the mass of the vehicle, and J its centroidal moment of inertia in the direction of yaw.

$$m(\dot{V} + \omega_y U) = \Sigma F_y \tag{3}$$
$$J\dot{\omega}_y = \Sigma M_y \tag{4}$$

Both the bicycle model and the handling model's dynamics are represented by these equations. However, the difference lies in the formulation of total lateral force and yaw moment, ΣF_y and ΣM_y respectively. The bicycle model, neglecting the effect of weight transfer due to cornering, assumes that the left and right tires generate the same force. The lateral force generated by the front and rear axle of the vehicle is described

by Eqn. (5). Both the bicycle and handling models of planar vehicle dynamics assume small steering angle ($\delta << 1$) in their formulation. Thus

$$F_f = F_{L1} + F_{R1} = C_f \alpha_f, F_r = F_{L2} + F_{R2} = C_r \alpha_r \tag{5}$$

where

$$\alpha_f = \delta - \frac{V + a\omega_y}{U}, \alpha_r = \frac{b\omega_y - V}{U}$$

A summation of lateral axle forces and moments generates the following terms:

$$\Sigma F_y = C_f \left(\delta - \frac{V + a\omega_y}{U} \right) + C_r \left(\frac{b\omega_y - V}{U} \right) \tag{6}$$

$$\Sigma M_y = aC_f \left(\delta - \frac{V + a\omega_y}{U} \right) - bC_r \left(\frac{b\omega_y - V}{U} \right). \tag{7}$$

Eqns. (3) coupled with (6) and (4) coupled with (7) fully represent the dynamical equations of motion of the two degree of freedom bicycle model. The static parameters C_f and C_r are selected to ensure that the bicycle model has slight understeer characteristics, and is thus stable regardless of forward operating velocity [12]. This model neglects variation in performance due to weight transfer, and will serve as the reference model for simulation studies.

The handling model of planar vehicle dynamics statically determines lateral weight transfer as a function of center of gravity height, vehicle mass, track width and instantaneous lateral acceleration. The weight transfer is split between the front and rear axles of the vehicle in proportion to front and rear roll stiffnesses, which are a function of suspension kinematics and compliance.

Revisiting Figure 1, it is seen that the tire normal loading has a direct influence on lateral force generation during cornering, and that this relation is non-linear with a negative curvature. Herein lies the crux of the problem. Imagine that the figure represents the current operation of the front axle of the bicycle model, with $\star$ representing the nominal front axle normal loading. As no weight transfer occurs, both the front left and front right tires will generate the same lateral force, as formalized by Eqn. (5). Conversely, the handling model does encompass weight transfer, and some amount of normal loading will transfer between the left and right tires of the vehicle. Assuming a steady-state left turn, the normal loading of the front left tire will be reduced from $\star$ and the normal loading of the right front tire will increase from $\star$ by that same amount. Thus, the total nominal weight of the front axle has remained constant, only its distribution between the front tires has changed. Summing the force generated by both front tires of the bicycle model, operating at $\star$, and both front tires of the handling model operating equidistant to the left and right of $\star$ we note the following: *the total cornering force of the front tires predicted by the handling model is less then that of the bicycle model*. The handling model is indicative of physical

vehicle planar dynamics, as physical tires adhere to the non-linearity in force generation with respect to normal loading exhibited in Figure 1.

It is the goal of this work to develop a control philosophy which augments the normal loading of the controlled vehicle so that its yaw-rate may approach the yaw-rate of the stable two degree of freedom bicycle model. In addition, it is necessary that this control intervention does not effect the already desirable roll/heave/pitch chassis dynamics.

III. PROPOSED CONTROL ARCHITECTURE

The proposed control architecture is shown in Figure 3. Similar control architecture was used in [13] for the control of planar dynamics of a wheel motored vehicle. It is used here to allocate normal force augmentation at the corners of the vehicle. Driver commands such as pedal position and steering wheel angle are input to a 2 degree-of-freedom reference bicycle model which returns the desired yaw rate. The bicycle model is also capable of generating a desired lateral velocity. However unlike yaw rate, lateral velocity cannot be directly measured. Therefore, all controllers presented in this work will only attempt to track the reference model yaw rate using feedback from onboard yaw rate sensors.

The reference tracking controller interfaces with the control allocation scheme in an attempt to align the actual vehicle yaw rate with that of the reference model. Any controller capable of robustly driving error signals toward zero is a qualified candidate. For the purpose of this study, control allocation is achieved by both optimal and sub-optimal methodologies. The usage of the terms optimal and sub-optimal will be discussed in the relevant sections.

Finally, the low-level controllers combine the normal force modulation request from control allocation with the primary objective of isolating the chassis from road disturbance to control the suspension actuators. For simulation purpose, active suspension is implemented in parallel with passive spring/damper suspension. It is assumed that the passive suspension has been designed to produce desirable chassis motion. The active suspension elements are driven by the normal force augmentation requested from control allocation, subjected to the motion ratio introduced in Eqn.(1).

A. Control Allocation

The objective in this section is to allocate normal force augmentation at each corner of the vehicle without upsetting the chassis attitude, while generating appropriate yaw moment to improve handling. In order to achieve this, it is required that the net change in roll moment, pitch moment, and total vertical force due to the normal force modulations be zero. That is

$$\Sigma \Delta M_{\text{roll}} = \Delta F_{z_{R1}} + \Delta F_{z_{R2}} - \Delta F_{z_{L1}} - \Delta F_{z_{L2}} = 0 \quad (8)$$

$$\Sigma \Delta M_{\text{pitch}} = b(\Delta F_{z_{L2}} + \Delta F_{z_{R2}}) - a(\Delta F_{z_{L1}} + \Delta F_{z_{R1}}) = 0 \quad (9)$$

$$\Sigma \Delta F_z = \Delta F_{z_{L1}} + \Delta F_{z_{R1}} + \Delta F_{z_{L2}} + \Delta F_{z_{R2}} = 0. \quad (10)$$

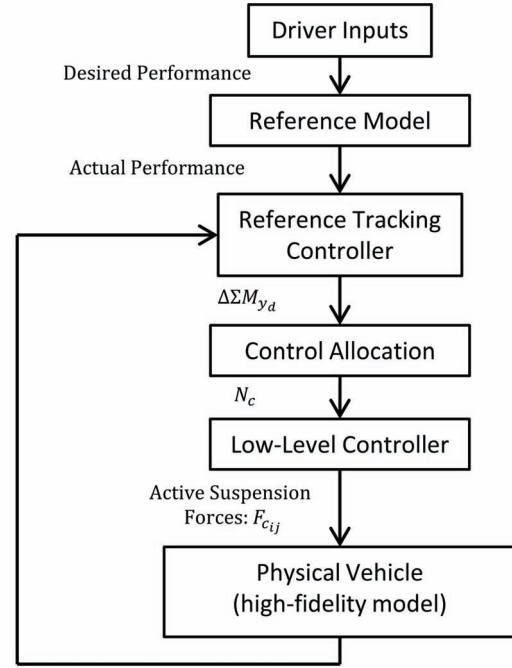Solving the above equations for $\Delta F_{z_{ij}}$ yields a particular constraint on the normal forces;

Fig. 3. Block Diagram of Proposed Control Architecture

$$\Delta F_{z_{R1}} = \Delta F_{z_{L2}} = -\Delta F_{z_{L1}} = -\Delta F_{z_{R2}},$$

or

$$\Delta F_{z_{R1}} + \Delta F_{z_{L2}} = -\left(\Delta F_{z_{L1}} + \Delta F_{z_{R2}}\right) \triangleq N_c F_{z_{total}} \quad (11)$$

Thus, the feasible set is completely parametrized by a single modulation variable N_c which will be designed subsequently. The variable N_c can also be seen as a cross-weight transfer, which is used to dynamically modify the cross-weight of the vehicle in order to improve the handling performance. Cross-weight is a term used in motor racing which describes the proportion of the total vehicle weight resting on the right front (R1) and left rear (L2) tires[1]. This static adjustment, also known as wedge, changes the stability of the chassis in turns and is often expressed as a fraction of the vehicle weight:

$$CW\% = \frac{F_{z_{R1}} + F_{z_{L2}}}{F_{z_{total}}} \quad (12)$$

The force bias implied by added wedge is effective in creating the desired understeer or oversteer characteristics on circle or oval tracks, where all turns are in the same direction. For normal racetracks, static wedge is rarely used as it lends to asymmetric handling for left versus right-handed turns.

Thus, the wedge constraint in Eqn. (11) creates a dynamic cross weight transfer according to

---

[1]Interested readers can check the website "auto.howstuffworks.com/auto-racing/nascar/jobs/nascar-wedge-adjustment3.htm" for more information on cross weights

$$\Delta CW\% = N_c = \frac{\Delta F_{z_{R1}} + \Delta F_{z_{L2}}}{F_{z_{total}}}, \quad (13)$$

in that wedge is transfered, dynamically, from the cross weight $F_{z_{L1}} + F_{z_{R2}}$ to $F_{z_{R1}} + F_{z_{L2}}$ by an amount equal to N_c. The application of dynamic wedge using an active suspension makes it possible to effectively shift the weight distribution to suit the instantaneous driving situation. Actuator-specific limitations such as the rate and magnitude limitations on force delivery can be incorporated into an analysis and a trade-off between power usage and performance can be found.

1) Optimal Allocation: Here, the allocation variable N_c is determined in such a way as to generate the necessary yaw moment to drive the vehicle responses towards the reference model. The term optimal is used to describe this approach because it attempts to determine the best case control possible, without considering implementation issues. Most of the required signals cannot be obtained in practice. Although, the resulting controller is unrealizable, it is used in this paper to represent the best possible scenario, therefore serving as a benchmark for the subsequent realizable controller.

Summing moments about the center of gravity in Figure 2 with respect to augmented tire forces yields:

$$\Delta \Sigma M_y = \frac{w}{2}(-\Delta F_{x_{L1}}^* + \Delta F_{x_{R1}}^* - \Delta F_{x_{L2}} + \Delta F_{x_{R2}})$$
$$+ a(\Delta F_{y_{L1}}^* + \Delta F_{y_{R1}}^*) - b(\Delta F_{y_{L2}} + \Delta F_{y_{R2}}) \quad (14)$$

$$\Delta F_{x_{ij}}^* = \Delta F_{x_{ij}} \cos \delta - \Delta F_{y_{ij}} \sin \delta \quad (15)$$
$$\Delta F_{y_{ij}}^* = \Delta F_{y_{ij}} \cos \delta + \Delta F_{x_{ij}} \sin \delta \quad (16)$$

$$\Delta F_{x_{ij}} = \frac{\partial F_{x_{ij}}}{\partial F_{z_{ij}}} \Delta F_{z_{ij}}, \Delta F_{y_{ij}} = \frac{\partial F_{y_{ij}}}{\partial F_{z_{ij}}} \Delta F_{z_{ij}} \quad (17)$$

Eqns. (14-17) represent how augmenting normal loading generates a change in yaw moment. By adhering to the control philosophy dictated in Eqn. (11) we may augment the generated yaw moment while avoiding upsetting chassis roll-heave-pitch dynamics. The resulting linear control effectiveness relation is shown in Eqns. (18,19). The partial derivative components of Eqn. (19) were generated by differentiating the Pacejka Magic Formula [10] equations of longitudinal and lateral force generation with respect to normal force. As previously discussed, these partial derivative terms could not be accurately known during vehicle operation, and the optimal control scenario presented is to serve as a benchmark for controller performance evaluation.

$$\Delta \Sigma M_y = B_M N_c \quad (18)$$

$$B_M = [(\frac{w}{2}\frac{\partial F_{x_{L1}}}{\partial F_{z_{L1}}} - a\frac{\partial F_{y_{L1}}}{\partial F_{z_{L1}}}) + (\frac{w}{2}\frac{\partial F_{x_{R1}}}{\partial F_{z_{R1}}} + a\frac{\partial F_{y_{R1}}}{\partial F_{z_{R1}}})$$
$$(-\frac{w}{2}\frac{\partial F_{x_{L2}}}{\partial F_{z_{L2}}} - b\frac{\partial F_{y_{L2}}}{\partial F_{z_{L2}}}) + (-\frac{w}{2}\frac{\partial F_{x_{R2}}}{\partial F_{z_{R2}}} + b\frac{\partial F_{y_{R2}}}{\partial F_{z_{R2}}})] \quad (19)$$
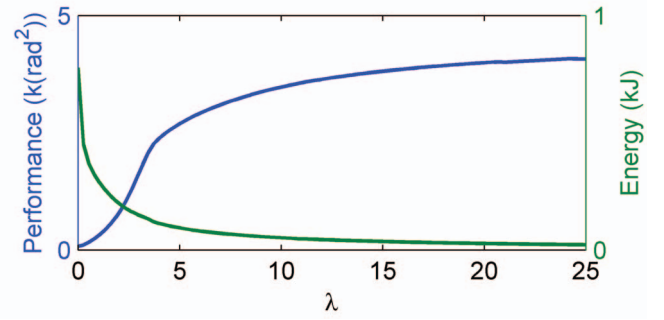

Fig. 4. Active Suspension System Total Energy Consumption and RMS Yaw Rate Tracking Error as a Function of λ Measured During Sine-with-Dwell Maneuver.

The objective function to be minimized is then given in Eqn. (20), where cross-weight modulation N_c is the decision variable. The first Euclidean norm of the objective function represents irritation resulting from a discrepancy between desired yaw moment augmentation ($\Delta \Sigma M_{yd}$) and actual yaw moment augmentation ($B_M N_c$). The second Euclidean norm term represents Tikhonov regularization while the final term provides a means of smoothing the allocation output [14].

$$f_o(N_c) = ||B_M N_c - \Delta \Sigma M_{yd}||_2^2$$
$$+ \lambda ||N_c||_2^2 + \zeta ||N_c(k) - N_c(k-1)||_2^2. \quad (20)$$

The scalar parameters λ and ζ allow for scaling between the three objective terms to be minimized, and are available to the calibration engineer for tuning system performance. Increasing λ penalizes the magnitude of N_c, thus reducing the total active suspension system energy. Based on the sine-with-dwell simulation study discussed in Section IV, the parametric results highlighted in Figure 4 were generated. The reduction in system energy resulting from increased values of λ came at the cost of system performance. Intrinsic constraints on actuator power are embedded in the objective function, in the form of the weighting terms λ and ζ. Increasing λ limits the force magnitude whereas ζ limits actuator rate. Larger values of ζ increasingly penalize N_c which vary greatly from their previous value, and thus smooth the request made by the control allocation.

Eqn. (20) represents a quadratic objective function with no explicit constraints, thus its minimum may be evaluated analytically. However, if the actuator magnitude or rate constraints required explicit formulation, the problem could be reworked in the constrained quadratic programming framework and solved using iterative techniques [15].

2) Sub-Optimal Control Allocation: To allow for realtime implementation, the partial derivative terms of Eqn. (19) can be replaced by estimable linear approximations as shown in Eqn. (21).

4089

$$\hat{B} = [(\frac{w}{2}\hat{N}_{x_{L1}} - a\hat{N}_{y_{L1}}) + (\frac{w}{2}\hat{N}_{x_{R1}} + a\hat{N}_{y_{R1}})$$
$$(-\frac{w}{2}\hat{N}_{x_{L2}} - b\hat{N}_{y_{L2}}) + (-\frac{w}{2}\hat{N}_{x_{R2}} + b\hat{N}_{y_{R2}})], \quad (21)$$

with

$$\hat{N}_{k_{ij}} = \frac{\hat{F}_k}{\hat{F}_{z_{ij}}}, \quad k \in \{x, \; y\}, i \in \{L, \; R\}, j \in \{1, \; 2\}$$

The sub-optimal problem is then formulated as a minimization of the objective function:

$$f_o(N_c) = ||\hat{B}_M N_c - \Delta\Sigma M_{y_d}||_2^2$$
$$+ \lambda||N_c||_2^2 + \zeta||N_c(k) - N_c(k-1)||_2^2, \quad (22)$$

B. Robustness Analysis

In this section, the robustness of yaw rate tracking performance to the estimation error inherent in sub-optimal control allocation described in the previous section is examined. Suppose N_c^* is the solution of the optimization problem in Eqn. (22), and $\varepsilon(N_c^*) \triangleq [\varepsilon_1(N_c^*), \; \varepsilon_2(N_c^*)]^T$ is the resulting mismatch between the actual generalized virtual forces and the ones due to the reference bicycle model. Then, the planar dynamical equations are given by

$$\Sigma F_y(N_c^*) = m\left(\dot{V} + \omega_y U\right) \quad (23)$$
$$\Sigma M_y(N_c^*) = J\dot{\omega}_y, \quad (24)$$

where

$$\Sigma F_y(N_c^*) = \varepsilon_1 + C_f\left(\delta - \frac{V + a\omega_y}{U}\right) + C_r\left(\frac{b\omega_y - V}{U}\right)$$
$$\Sigma M_y(N_c^*) = \varepsilon_2 + aC_f\left(\delta - \frac{V + a\omega_y}{U}\right) - bC_r\left(\frac{b\omega_y - V}{U}\right)$$

It is important to note that the cornering stiffnesses C_f, C_r, and the distances a, b are only parameters of the reference bicycle model and do not represent any approximation of the actual system.

Also, let

$$\mathbf{e} = \begin{bmatrix} V - V_r \\ \omega_y - \omega_{y_r} \end{bmatrix} \quad (25)$$

be the error between the responses of the planar dynamics in Eqns. (23) and (24) and the reference model ($\varepsilon_1 = \varepsilon_2 = 0$) with lateral velocity V_r and yaw rate ω_{y_r}. Then the error dynamics are written as

$$\dot{\mathbf{e}} = A_r\mathbf{e} + \varepsilon(N_C^*), \quad (26)$$

where

$$A_r = \begin{bmatrix} -\frac{C_f + C_r}{mU} & \frac{bC_r - aC_f}{mU} - U \\ \frac{bC_r - aC_f}{JU} & -\frac{a^2C_f + b^2C_r}{JU} \end{bmatrix}. \quad (27)$$

Thus, as shown in Eqn. (26), the estimation error associated with the sub-optimal control allocation becomes a disturbance
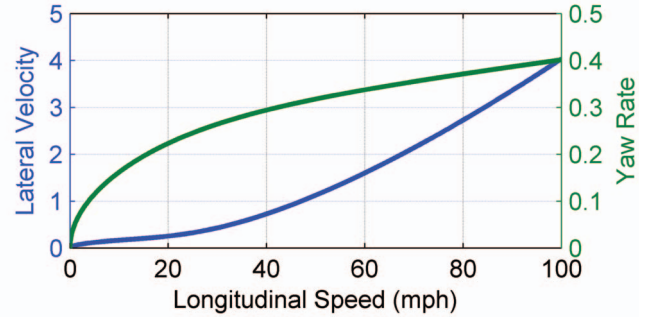

Fig. 5. $\mathcal{H}_2$ Gains of Lateral Velocity and Yaw Rate Errors

driving the error dynamics. Figure 5 shows the $\mathcal{H}_2$ gains[2] of the error dynamics as a function of the forward speed. It is seen that the performance degradation as result of the sub-optimal estimation errors increases with increasing forward speed, with the yaw rate approximately 10 times less sensitive to the estimation errors as the lateral velocity. It is thus confirmed that augmenting cross-weight is a robust method of tracking desired yaw rate.

IV. SIMULATION RESULTS

Discrete realizations of the two aforementioned control systems were implemented in MATLAB/Simulink™ environment and implemented on a CarSim©high-fidelity vehicle model. In each case, the vehicle being represented is a typical D-segment automobile (e.g., Toyota Camry, Honda Accord or Chevrolet Impala). Each control system operated with a rate of $100Hz$. The simulated vehicles were subjected to an open-loop sine-with-dwell steering maneuver based on the U.S. Department of Transportations electronic stability control systems testing method FMVSS-126c while traveling at 80kph (about 50mph).

Figure 6 highlights the yaw rate and lateral velocity error of the two controlled vehicles as compared with those of the 2 degree-of-freedom reference bicycle model. The error signals of a vehicle conducting the same maneuver with no active suspension system intervention are also plotted for the sake of comparison. As is evident from the figure, without active suspension intervention this vehicle was unable to maintain stable operation. Conversely, the two controlled vehicles were able to stabilize the vehicle subject to the aggressive steering maneuver.

Figure 7 presents the cross-weight ratios defined in Eqn. (12) as well as the total absolute power required by the active suspension systems for the vehicles completing the sine-with-dwell maneuver. It is evident that the active suspension systems augment the cross-weight greatly as compared with its

[2]The $\mathcal{H}_2$ gain of the stable, strictly proper dynamical system

$$G : \begin{cases} \dot{x} = Ax + Bu \\ y = Cx \end{cases}$$

is given by $||G||_2 = \sqrt{||C^T PC||_F}$, where $P = P^T > 0$ is the unique solution to the Lyapunov equation $AP + PA^T + I = 0$.
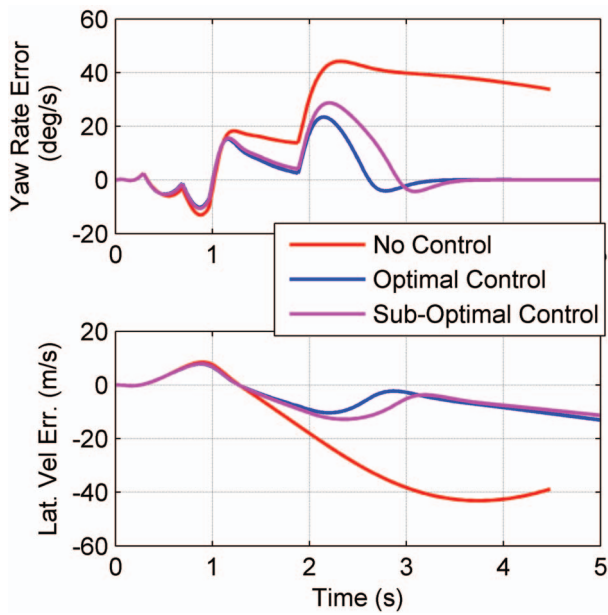
Fig. 6. Top: Yaw Rate of Vehicles in Response to Sine-with-Dwell Open Loop Steering Input. Bottom: Measured Normal Loading Cross-Weight Ratio During Sine-with-Dwell Maneuver.
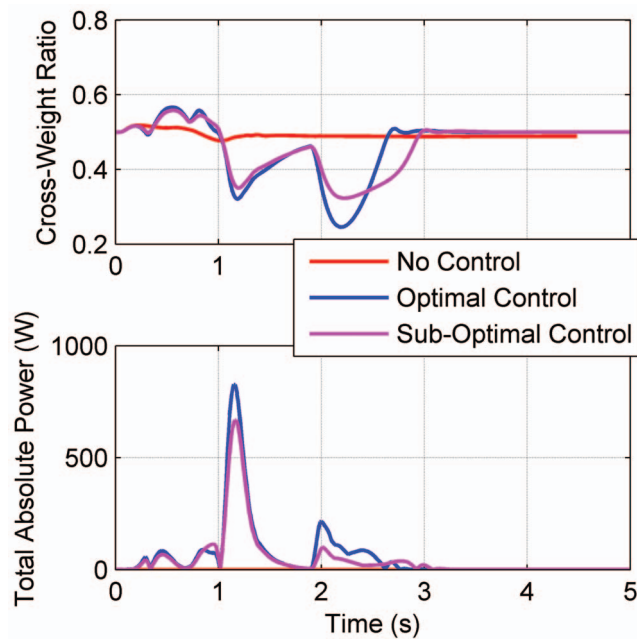

Fig. 7. Top: Measured Normal Loading Cross-Weight Ratio During Sine-with-Dwell Maneuver. Bottom: Total Absolute Power Required by Active Suspension Systems

passive evolution, as shown by the *No Control* study. However, the total power required to do so appears to be feasible. As was shown in Figure 4, this power requirement can be made arbitrarily small at the cost of increased yaw rate tracking error.

V. CONCLUSION

A novel technique for utilizing active suspension elements to dynamically augment vehicle cross-weight without upsetting chassis roll/heave/pitch dynamics is presented. It is shown that augmenting tire normal loading in this fashion affords control over planar vehicle dynamics. Two methods of control allocation are proposed for yaw rate tracking to enhance vehicle performance. First an optimal, albeit impractical, control allocation problem is formulated to provide a benchmark for subsequent controller performance. Simplifying assumptions are made to generate a practical sub-optimal variant of this controller. A robustness analysis is conducted to prove the stability of the sub-optimal system as a result of its simplifying assumptions – it was shown that the sub-optimal control system can robustly track vehicle yaw rate.

The two developed controllers were implemented on a CarSim© high-fidelity vehicle model undergoing an aggressive sine-with-dwell maneuver. A vehicle without control intervention was shown to lose control, while the two implemented controllers were able to stabilize the vehicle. Additionally, it was shown that the power requirements of the system are not extraordinary, and can be managed by tuning the performance gains of the respective control systems.

REFERENCES

[1] D. Karnopp, "Active damping in road vehicle suspension systems," *Vehicle System Dynamics*, vol. 12, no. 6, pp. 291–311, 1983.
[2] K. A. Unyelioglu, U. Ozguner, T. Hissong, and J. Winkelman, "Wheel torque proportioning, rear steering, and normal force control: a structural investigation," *Automatic Control, IEEE Transactions on*, vol. 42, no. 6, pp. 803–818, 1997.
[3] G. Mastinu, E. Babbel, P. Lugner, D. Margolis, P. Mittermayr, and B. Richter, "Integrated controls of lateral vehicle dynamics," *Vehicle System Dynamics*, vol. 23, no. S1, pp. 358–377, 1994.
[4] D. Karnopp, M. J. Crosby, and R. Harwood, "Vibration control using semi-active force generators," *Journal of Engineering for Industry*, vol. 96, no. 2, pp. 619–626, 1974.
[5] M. Blank and D. Margolis, "The effect of normal force variation on the lateral dynamics of automobiles," *Development*, vol. 2012, pp. 02–20, 1996.
[6] T. Shim and D. Margolis, "Dynamic normal force control for vehicle stability enhancement," *International journal of vehicle autonomous systems*, vol. 3, no. 1, pp. 1–14, 2005.
[7] C. Smith, *Tune to Win*. Fallbrook CA: Aero, 1978.
[8] T. D. Gillespie, "Wheel hop resonances," in *Fundamental of Vehicle Dynamics*. Warrendale PA: SAE, 1992.
[9] E. Sevin and W. D. Pilkey, "Optimum shock and vibration isolation," DTIC Document, Tech. Rep., 1971.
[10] H. B. Pacejka, "Chapter 4 - semi-empirical tyre models," in *Tyre and Vehicle Dynamics (Second Edition)*, H. B. Pacejka, Ed. Oxford: Butterworth-Heinemann, 2006, pp. 156–215.
[11] L. R. Ray, "Nonlinear tire force estimation and road friction identification: simulation and experiments," *Automatica*, vol. 33, no. 10, pp. 1819–1833, 1997.
[12] D. Karnopp, "Body-fixed coordinate formulation," in *Vehicle Stability*. Marcel Dekker, 2004, pp. 106–109.
[13] S. Varnhagen, M. O. Anubi, and D. Margolis, "Development of realizable and adaptive wheel torque allocation for the control of planar vehicle dynamics," in *Dynamic Systems and Control*, ASME, Ed., San Antonio, Texas, 2014.
[14] S. Boyd and L. Vandenberghe, "Regularization," in *Convex Optimization*. Cambridge University Press, 2004, pp. 306–308.
[15] L. Wang, "Hildreth's quadratic programming procedure," in *Model Predictive Control System Design and Implementation Using MATLAB*, 2009, pp. 63–68.